

Prescribed burns as a tool to mitigate future wildfire smoke exposure: Lessons for states and rural environmental justice communities

¹Makoto M. Kelp, ²Matthew Carroll, ³Tianjia Liu, ⁴Robert M. Yantosca, ⁵Heath E. Hockenberry, ⁴Loretta J. Mickley

¹Department of Earth and Planetary Sciences, Harvard University, Cambridge, MA 02138, USA

²United States Forest Service, Bar Harbor, ME 04609, USA

³Department of Earth System Science, University of California, Irvine, Irvine, CA 92697, USA

⁴John A. Paulson School of Engineering and Applied Sciences, Harvard University, Cambridge, MA 01238, USA

⁵National Weather Service, Boise, Idaho, 83705, USA.

Corresponding author: Makoto M. Kelp (mkelp@g.harvard.edu)

Key Points:

- The West Coast both experiences the largest smoke exposures and contributes most to the burden of smoke PM_{2.5} in the western US
- Applying prescribed burns on the coast yields large benefits for the West, while doing so in other states has relatively smaller impacts
- Larger prescribed burns may reduce smoke impacts from future large wildfires, but few such burns have occurred in key areas

Abstract:

Smoke from wildfires presents one of the greatest threats to air quality, public health, and ecosystems in the United States, especially in the West. Here we quantify the efficacy of prescribed burning as an intervention for mitigating smoke exposure downwind of wildfires across the West during the 2018 and 2020 fire seasons. Using the adjoint of the GEOS-Chem chemical transport model, we calculate the sensitivities of population-weighted smoke concentrations in receptor regions, including states and rural environmental justice communities, to fire emissions upwind of the receptors. We find that the population-weighted smoke exposure across the West during the September 2020 fires was $44 \mu\text{g}/\text{m}^3$ but would have been 20-30% greater had these wildfires occurred in October or November. We further simulate a set of prescribed burn scenarios and find that controlled burning interventions in northern California and the Pacific Northwest could have reduced the population-weighted smoke exposure across the western United States by $21 \mu\text{g}/\text{m}^3$ in September 2020, while doing so in all other states would have reduced smoke exposure by only $1.5 \mu\text{g}/\text{m}^3$. Satellite records of large, prescribed burns (>1000 acres, or 4 km^2) reveal that northern California and western Oregon conducted only seven such prescribed fires over a 6-year period (2015-2020), even though these regions have a disproportionate impact on smoke exposure for rural environmental justice communities and population centers across the West. Our analysis suggests that land managers should prioritize northern California and the Pacific Northwest for prescribed burns to mitigate future smoke exposure.

Plain Language Summary

Catastrophic wildfires pose substantial risk to public health, infrastructures, and ecosystems in the western United States. As these large and costly wildfires become more common, methods to identify locations for prescribed burning are needed to mitigate impacts on affected populations and ecosystems. Here we investigate the effectiveness of prescribed burning for abating potential wildfire smoke exposures in states and rural environmental justice communities across the western United States during the destructive 2018 and 2020 fire seasons. We find that due in part to prevailing wind patterns, wildfires in the coastal states contribute more to overall smoke exposure in the West compared to wildfires in other states in both 2018 and 2020. We show that implementing prescribed burns in the heavily forested Northern California and the Pacific Northwest would yield large net benefits for the entire western United States, while doing so in other states would have relatively smaller impacts. Our work suggests that land managers should prioritize northern California, western Oregon, and eastern Washington for prescribed burns to mitigate future smoke exposure as these regions have a disproportionate impact on smoke exposure for rural environmental justice communities and population centers across the West.

Keywords: wildfires, prescribed fires, fine particulate matter ($\text{PM}_{2.5}$), environmental justice

Introduction:

Given decades of successful air pollution regulations coupled with the dramatic increase in fire activity across the western United States (Abatzoglou and Williams, 2016), smoke particulate matter (PM_{2.5}) from wildfires presents one of the greatest threats to air quality in the United States, especially in the West (Childs et al., 2022; Larsen et al., 2018). PM_{2.5} can penetrate deep into the lungs, leading to an array of health effects, including pulmonary disease, stroke, and premature death (Landguth et al., 2020; Liu et al., 2017). Land managers in the western United States are faced with the challenge of deciding how to deploy limited resources to protect citizens from encroaching wildfires in the wildland–urban interface (WUI). These personnel are increasingly seeking opportunities to expand the scope of prescribed burning to minimize the socio-ecological impacts of large wildfires. However, the potential to avert widespread smoke exposure from future wildfires is not taken into consideration when planning prescribed fires (Sutherland and Edwards, 2022). Although prescribed burning worsens air quality in specific locations on short-term time scales, it may have the capability to reduce community smoke exposure at large scales in the Western United States. In August 2022, Congress passed the Inflation Reduction Act, which designates nearly \$2 billion toward the reduction of hazardous fuels through the use of prescribed burns and other measures (H.R.5376). Here we estimate the efficacy of prescribed burning as a land management intervention for mitigating smoke exposure in population centers and rural environmental justice communities downwind of potential wildfires across the western United States.

An increased urgency exists for evaluating the net benefits of prescribed fires over a broad range of ecosystems in the West. A warming climate, a legacy of fire suppression, and population growth in the WUI all increase the likelihood of large wildfires in the western United States causing significant environmental damage (FERA, 2020). Sedimentary charcoal records indicate widespread indigenous fire activity in the western United States 500-1000 years before present, suggesting a large “fire deficit” in the present-day landscape (Marlon et al., 2012). Although prescribed burning has been used as a land management tool for centuries, limited information exists that allows for a comparison of smoke exposure from prescribed fires and wildfires in the western United States. Indigenous communities in the West and worldwide have traditionally used prescribed burning to return nutrients to the soil and to limit the frequency of large fires (Lake et al., 2017; Lake and Christianson, 2019). In the United States, controlled burns for agricultural clearing and habitat management dominate the acres burned in the Southeast and East, while uncontrolled wildfires dominate in the West (Baker et al., 2020). However, the West experiences a larger burden of smoke PM_{2.5} than elsewhere in the contiguous United States, because wildfires exhibit greater fuel consumption than prescribed fires (Baker et al., 2020). Public acceptance of prescribed fires in the West is less widespread in part due to concerns over escaped fires and the potential air quality impact of smoke (Kolden, 2019). Furthermore, most scientific evidence of the net benefits of prescribed burning in the West derive from a limited number of case studies (Jaffe et al., 2020; US EPA, 2021; Vaillant et al., 2009).

Wildfire data with high spatial and temporal resolution have enabled recent investigation of the impacts of smoke on urban air quality (O’Dell et al., 2022; Reid et al., 2021), while the smoke effects on rural environmental justice communities may have been overlooked. Recently, the proliferation of high-resolution satellite data has transformed how air pollution is tracked and

interpreted. With the launches of TROPOMI in 2017 and the geostationary satellite constellation (GEMS in 2020, Sentinel-4 and TEMPO to be launched in 2023), dense, continuous observations of air quality and wildfires across the Earth are becoming available (Griffin et al., 2021; Kim et al., 2020; Torres et al., 2020). Concurrently, the spatial resolutions of air quality models have continued to approach finer scales (Bindle et al., 2021; Eastham et al., 2018). Machine-learning approaches have inferred levels of surface pollution where no measurements exist (Di et al., 2019; Pendergrass et al., 2022), downscaled PM_{2.5} observations to the hyperlocal (<50 m) scale (Yang et al., 2020), and incorporated high-resolution wildfire smoke plumes into air quality datasets (L. Li et al., 2020). In addition, citizen-science and low-cost sensor networks are increasing the urban spatiotemporal coverage of air quality observations to study wildfire smoke exposure in the West (Bi et al., 2022; Liang et al., 2021).

Such progress in spatial resolution has led to an increased focus on urban centers at the expense of rural, at-risk communities (Pellow, 2016). For example, outside of metropolitan hubs, the Central Valley in California and Central/Eastern Washington State have large populations of non-white Hispanic agricultural workers who are disproportionately affected by smoke PM_{2.5} as an occupational hazard (Cedar River Group, 2012; Chandrasekaran, 2021; Garcia 2007; Marlier et al., 2022), but whose PM_{2.5} exposure is not well monitored (deSouza and Kinney, 2021; Kelp et al., 2022). The Navajo nation, a Native American reservation in the Southwest, is the largest land area held by an indigenous tribe in the United States (Guiterman et al., 2019). People living on the reservation typically experience lower annual-average PM_{2.5} exposure compared to other racial minority groups in the western United States due to the rural location (Jbaily et al., 2022). However, indigenous groups such as the Navajo experience higher rates of diseases linked to air pollution exposure (Ospina et al., 2012) and in turn are likely more susceptible to the long-range transport of smoke to tribal lands.

A multitude of studies have investigated wildfire activity in the western United States, including wildfire trends (Abatzoglou and Williams, 2016; McClure and Jaffe, 2018; O'Dell et al., 2019), smoke transport (Barbero et al., 2014; Wu et al., 2012), and the health impacts of smoke exposure (Magzamen et al., 2021; Reid et al., 2016). Relatively few studies, however, have examined the role of meteorology to modulate smoke exposure on the populations downwind or the efficacy of prescribed burns as a policy intervention. We adopt an existing framework connecting fire emissions with transport to calculate population-weighted smoke exposure for an array of target regions (Kim et al., 2015; Koplitz et al., 2016; Marlier et al., 2019). To date, this framework has been limited to case studies in Southeast Asia. To our knowledge, there exist no systematic studies examining the potential of prescribed burns to reduce population exposure to wildfire smoke.

In this study, we develop an approach to predict at the state level where prescribed fires and other fire management approaches would yield the greatest benefit to air quality downwind of potential large wildfires in the western United States. Our approach integrates (1) information on fire emissions related to land use in the western United States, (2) the transport of smoke to downwind regional population centers in states and rural environmental justice communities, and (3) the resultant population-weighted exposure. We simulate the transport of smoke PM_{2.5} for the 2018 and 2020 fire seasons in the western United States and quantify how meteorological variability can modulate smoke exposure. We also quantify the effectiveness of prescribed

burning as a land management tool in the West by investigating the smoke exposure effects of applying in-state and out-of-state prescribed burns, and we compare these hypothetical burns to historical records of prescribed burning.

Methods:

2.1 Historical Fire Emissions

We use monthly-averaged $0.25^\circ \times 0.25^\circ$ emissions estimates from the Global Fire Emissions Database version 4s (GFED4s; van der Werf et al., 2017) with $1 \text{ km} \times 1 \text{ km}$ burned area (MCD64A1) measurements from MODerate resolution Imaging Spectroradiometer (MODIS) on board the Aqua and Terra satellites (Giglio et al., 2016; van der Werf et al., 2017). The fire emissions are based on observed relationships between burned area and fuel load consumption assumed from the CASA biogeochemical model (Randerson et al., 2009). In GFED4s, fuel consumption is defined as the amount of biomass, coarse and fine litter, and soil organic matter consumed per unit area burned and is the product of fuel and combustion completeness. We choose the monthly timescale because GFED from 2017 onwards is a preliminary dataset, using the linear relationship between historical GFED emissions and active fire detections to estimate daily emissions (Mu et al., 2011). The daily partitioning of monthly GFED4s emissions relies on using the daily variability in active fire counts and burned area, which may not accurately reflect the daily variability in emissions due to changes in fire intensity and sub-grid cell variability in fuel load (Mu et al., 2011).

We use monthly GFED4s fire emissions for the 2018 and 2020 fire seasons (July–November) in the western United States due to the high number of fires detected and the large extent of area burned during those years. The Camp Fire of November 2018 was one of the most damaging environmental events in Northern California’s history (Brewer and Clements, 2020; Rooney et al., 2020). The fire spanned 620 km^2 in area, and total economic damages were estimated at \$16.5 billion, in addition to over \$150 million in fire suppression costs (Bay City News, 2018). In addition, the Martin Fire in northern Nevada occurred from July to August in the 2018 fire season, which burned a total area of 1770 km^2 and was the largest fire in Nevada’s history. Wyoming also had over 240 km^2 burned in the Bridger-Teton National Forest in September of 2018. In the 2020 fire season, several major wildfires ignited in the West and burned over $41,000 \text{ km}^2$ of land, causing nearly \$20 billion in economic damages, in addition to \$3.4 billion in fire suppression costs (Geographic Area Coordination Center, 2020). Colorado experienced the three largest fires by burned area in its state’s recorded history during this season, resulting in over $2,100 \text{ km}^2$ burned (Colorado Division of Fire Prevention and Control, 2022).

The 2018 and 2020 fire seasons were the most destructive in recent decades, with most of the fire emissions originating from coastal states. To better quantify the smoke impacts from other states in the West, we also include an analysis using GFED4s emissions from the following large fires in other years: (1) July 2007 for the Murphy Complex Fire in Idaho and the Milford Flat Fire in Utah, (2) June 2011 for the Wallow Fire in Arizona, (3) June 2012 for the Whitewater–Baldy complex Fire in New Mexico, and (4) July 2017 for the Lodgepole Complex Fire in Montana. These high-fire case studies are significant in the histories of each of these states and warrant analysis in addition to the 2018 and 2020 fire seasons.

2.2 GEOS-Chem Adjoint

The adjoint of the GEOS-Chem chemical transport model allows us to calculate the potential influence of fire emissions in each grid cell across the domain on population-weighted smoke exposure in specified receptor regions. The adjoint considers the advection, convection, and deposition processes in smoke plumes as they traverse the region. Following the approach of previous studies (Kim et al., 2015; Koplitz et al., 2016; Marlier et al., 2019), we use the adjoint of the GEOS-Chem v8-02-01 (Bey et al., 2001; Henze et al., 2007) to quantify these source-receptor relationships. GEOS-Chem is driven by GEOS-FP assimilated meteorology from the NASA Global Modeling and Assimilation Office. Simulations have $0.25^\circ \times 0.3125^\circ$ horizontal resolution over the nested North America domain (140° – 40° W, 10° N– 70° N). The method takes into account the spatiotemporal distribution of smoke plumes and generates monthly mean gridded sensitivities, hereafter referred to as adjoint sensitivities, in units of $\text{mg m}^{-3}/\text{g m}^{-2} \text{ s}^{-1}$. We define smoke as the primary $\text{PM}_{2.5}$ emitted by fires in the form of organic carbon and black carbon (OC+BC), as described by Wang et al., 2011. Multiplication of the adjoint sensitivities by the fire emissions yields smoke exposure in receptor regions for any fire emissions scenario, as the relationship between emissions at the source and smoke exposure at the receptor is assumed to be linear (Kim et al., 2015). For population-weighted smoke exposures, we use population data for the year 2020 (CIESIN, 2018).

We select 11 state, regional, and rural environmental justice community receptors as shown in Table 1 and Figure 1. At the state-level, we choose eight receptors roughly aligned with the Geographic Area Coordination Centers (GACC, <https://gacc.nifc.gov>), which are areas designed to facilitate fire management and mobilization of fire suppression resources in the western United States. These seven receptors include Washington and Oregon (WA/OR); Nevada (NV); Montana, Wyoming, and Colorado (“Rockies”); Idaho and Utah (ID/UT); Arizona and New Mexico (“SouthWest”); Northern California (“NorCal”); and Southern California (“SoCal”). At the regional level, we create a single receptor that contains all the states listed above (“West”) to examine the population-weighted smoke exposure of fires collectively experienced by the entire western United States. Finally, we select three rural environmental justice communities, including counties in the Central Valley (“CVCal”), Central/Eastern Washington (“CEWA”), and the Navajo Nation (“NavN”) found in the Four Corners region. These rural receptors represent vulnerable communities with large nonwhite populations where exposure to urban air pollution is low, but which tend to experience outsized impacts from ecological disasters such as large wildfires (Davies et al., 2018). However, the CVCal does include multiple cities with populations larger than 500,000 people (Fresno, Bakersfield, Stockton, and Modesto).

Table 1. State and rural environmental justice community receptors.

Receptor Name	Receptor Area
ID/UT	Idaho and Utah
NV	Nevada
NorCal	Northern California – 48 counties north of 36° N
Rockies	Colorado, Montana, Wyoming
SoCal	Southern California – 10 counties south of 36° N
SouthWest	Arizona, New Mexico
WA/OR	Washington and Oregon
West	Arizona, California, Colorado, Idaho, Montana, Nevada, New Mexico, Oregon, Utah, Washington, Wyoming
CVCa	Central Valley, California (rural community)
CEWash	Central and Eastern Washington (rural community)
NavN	Navajo nation Indian reservation (rural community)

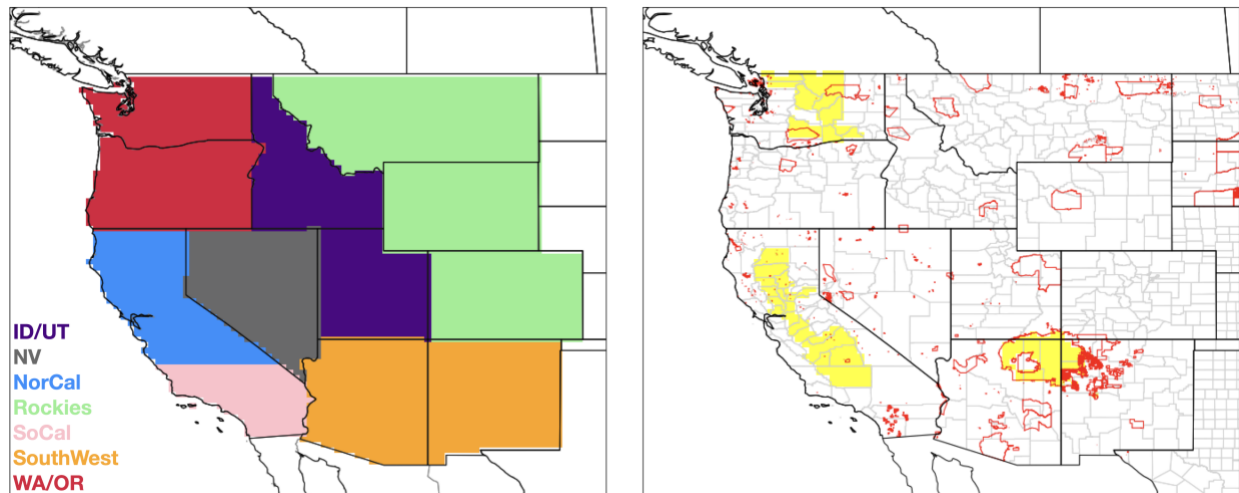


Figure 1. State and rural environmental justice community receptors at $0.25^\circ \times 0.3125^\circ$ resolution. The seven state-level receptors (left panel) are described in the text and Table 1. Overlaps of the receptors across state lines are an artifact of the unsymmetrical $0.25^\circ \times 0.3125^\circ$ grid. The three rural environmental justice receptors are shown in yellow (right panel). Counties in the right panel are outlined in grey and Native American territories in red.

2.3 Modulation of smoke exposure by meteorology

We first examine the potential of meteorology to suppress or amplify smoke exposures at downwind receptors. We calculate the adjoint sensitivities for all 11 receptors, given meteorological conditions for the July-November fire seasons in 2018 and 2020, yielding a set of monthly mean adjoint sensitivity maps spanning ten months total for each receptor across the two seasons. This approach allows us to focus on the monthly variation in meteorological processes which affect smoke transport to the receptors and the subsequent smoke exposure. We examine two scenarios. First, exposures in the “historical smoke” scenario are calculated by multiplying monthly mean fire emissions in the 2018 and 2020 fire seasons by the matching

monthly adjoint sensitivity – e.g., July 2018 fire emissions are multiplied by July 2018 adjoint sensitivity. This scenario attempts to capture what actually occurred. Second, exposures in the “maximum smoke” scenario are calculated by multiplying each season’s largest monthly-mean fire emissions by each of the five monthly adjoint sensitivities from July to November for that season. The months with the largest emissions for the latter scenario are November 2018 and September 2020. This hypothetical scenario tests what would happen if the worst-case smoke emissions in a season were paired with different meteorological conditions.

Our method isolates the role of meteorology in smoke transport from its role in fire ignition and allows us to discern the potential influence of meteorological processes to modulate smoke exposures in each receptor. In particular, the “maximum smoke” scenarios allow us to address the question: given a fixed set of emissions, how does meteorological variability within a fire season influence population-weighted smoke exposure? Our approach rests on observational evidence that a large portion of fires in the West are human caused (Abatzoglou and Williams, 2016; Balch et al., 2017; Hantson et al., 2022), implying a randomness to fire occurrence. In addition, across much of the West, seasonal area burned is mainly a function of seasonal meteorological variables such as temperature or rainfall (Yue et al., 2013). Such evidence suggests that significant fires may occur at any time during a given season. However, the resulting smoke exposure on populations downwind of fires depends on transport processes which typically vary on shorter timescales.

To broaden the scope of our study, we use the 2018 and 2020 adjoint sensitivities to analyze how these weather patterns affect the four high-fire case studies listed in Section 2.1. That is, we conduct an additional “maximum smoke” exposure analysis for large fires in ID/UT, SouthWest, and Montana. Although the sensitivities reflect 2018 and 2020 conditions and the high-fire cases occurred in earlier years, this analysis will nonetheless allow us to test how different meteorological conditions and emissions interact to affect population smoke exposure.

2.4 Prescribed fire scenarios for smoke exposures

We examine the efficacy of prescribed fires as a policy intervention for states in the western United States and compare scenarios of prescribed fires to historical records of prescribed burning locations. A study conducted by the United States Forest Service (USFS) on the Timber Crater 6 (TC6) Fire in Oregon suggests that effective prescribed burning and mechanical fuel treatments reduce tree densities by an average of 25% in ponderosa pine forests and 78% for lodgepole pine forests (US EPA, 2021). The USFS concluded that the legacy of fire suppression, fuel loading, and potential fire behavior in the TC6 Fire area are similar to these characteristics in other coniferous forests in the western United States (US EPA, 2021). Here, we assume that conducting prescribed burns within a receptor area would reduce the fuel load and thus subsequent wildfire emissions by 50% for all landscapes, including savannas and grasslands, in that receptor. For each state-level receptor, we apply a hypothetical 50% reduction in the fire emissions inside the receptor region and examine the consequent smoke PM_{2.5} exposure at that receptor and at all other receptors listed in Section 2.2. We apply this reduction to the high-emissions month of each fire season: November 2018 and September 2020. We acknowledge that the 50% cut in emissions is somewhat arbitrary. Nonetheless, this method captures the first order effects of prescribed burns on the emissions from subsequent wildfires and allows us to

calculate both the local and out-of-state smoke exposure impacts.

In addition, we compare our hypothetical modeling results with historical records of actual prescribed burn locations. We examine the Monitoring Trends in Burn Severity (MTBS) [<https://www.mtbs.gov/>] database over the course of 2015-2020. This step allows us to test whether recent prescribed burns have occurred in locations that may have helped prevent future large wildfires (Finco et al., 2012). MTBS accounts for only those prescribed fires that burned over 1000 acres ($\sim 4 \text{ km}^2$) and does not report smaller prescribed fires. To supplement MTBS, we also make comparisons to the National Fire Plan Operations and Reporting System (NFPORS) fuels treatment database, which is maintained by the US Department of the Interior collaboratively with the US Department of Agriculture. While NFPORS does report prescribed fires under 1000 acres, it does not include “pile burning,” the land management practice in which a prescribed fire is ignited onto piles of cut vegetation accumulated from fuel management activities. Pile burning may constitute a significant fraction of small, prescribed fires (Rhoades and Fornwalt, 2015). For NFPORS, the spatial information on area burned is limited before 2018, and so we restrict these comparisons from 2018 to 2020. We expect variation between MTBS (satellite-derived) and NFPORS (reports from land managers) due to the differing approaches of characterizing prescribed burns and levels of data quality control.

Results and Discussions:

3.1 Sensitivities and smoke exposure during wildfire season

For November 2018, our results show that the “historical smoke” scenario supports our hypothesis that the large fires of that month lead to the maximum population-weighted smoke exposures for the wildfire season. The top row of Figure 2 presents the “historical smoke” population-weighted exposure for each receptor for the 2018 and 2020 fire seasons. In November 2018, NorCal and the CVCal experience monthly-mean smoke exposures of $36 \mu\text{g}/\text{m}^3$ and $48 \mu\text{g}/\text{m}^3$, respectively. These modeled estimates agree well with observed monthly average $\text{PM}_{2.5}$ concentrations of $37\text{--}64 \mu\text{g}/\text{m}^3$ at EPA sites within northern California in that month (California Air Resources Board, 2021). However, the modeled smoke exposure in November 2018 is generally low outside of NorCal, with most receptors experiencing smoke $\text{PM}_{2.5}$ concentrations of less than $2 \mu\text{g}/\text{m}^3$. This disparity in exposure may be explained by the relatively stagnant meteorological conditions over NorCal in November 2018 that prevent dispersal of smoke from this region (Brewer and Clements, 2020). In November, average windspeeds off the coast and inland in NorCal are one-third those in the preceding months (Figure S1). We can further infer meteorology and transport processes driving the distribution of smoke by examining the average adjoint sensitivity of a receptor. A higher mean sensitivity suggests a larger effect by the weather (convection, advection, deposition), which in this case taken together with wind data (Figure S1, S2) implies more stagnant conditions. Conversely, a lower mean sensitivity suggests local emissions play a more important role in smoke concentrations. The mean NorCal adjoint sensitivity for November ($5492 \text{ mg m}^{-3}/\text{g m}^{-2} \text{ s}^{-1}$) is nearly double that of most other months in the 2018 fire season (July: 3120, August: 2902, September: 3309, October: $3916 \text{ mg m}^{-3}/\text{g m}^{-2} \text{ s}^{-1}$). Nevertheless, due to the large population centers found in NorCal, the population-weighted smoke exposure across the entire western United States is relatively large, at $8.3 \mu\text{g}/\text{m}^3$. In addition, we find elevated smoke exposures in August 2018 at multiple receptors, which we attribute to emissions from the Martin Fire in Nevada. However, the impact on the entire western United States is less pronounced in August, with a population-weighted smoke exposure of $5.2 \mu\text{g}/\text{m}^3$.

In contrast, in September 2020, all receptors experience relatively large smoke exposures in the historical scenario for the 2020 fire season. NorCal experiences a monthly mean smoke $\text{PM}_{2.5}$ concentration of $87 \mu\text{g}/\text{m}^3$, while the CVCal experiences an even higher $128 \mu\text{g}/\text{m}^3$, which is consistent with its closer proximity to fire emissions than NorCal (Figure S3). In addition, WA/OR has smoke exposures of $140 \mu\text{g}/\text{m}^3$, largely driven by the unprecedented extremes of fuel aridity and high winds that facilitated the spread of fires in Oregon (Abatzoglou et al., 2021). Although wildfires burned over $1,300 \text{ km}^2$ of land in CEWash, this receptor has a relatively low smoke exposure at $19 \mu\text{g}/\text{m}^3$ in September 2020, due to high winds pushing smoke rapidly eastward, limiting exposure levels. Finally, the large number and severity of wildfires along the West Coast in September 2020 yields a population-weighted smoke exposure of $44 \mu\text{g}/\text{m}^3$ for all states in the West. This monthly $\text{PM}_{2.5}$ average concentration exceeds the EPA’s annual ($15 \mu\text{g}/\text{m}^3$) and daily ($35 \mu\text{g}/\text{m}^3$) secondary $\text{PM}_{2.5}$ standards and corresponds to an air quality index (AQI) of 122 (“unhealthy for sensitive groups”). Generally, we observe that NorCal and WA/OR experience the largest population-weighted smoke exposures in the West in September 2020.

The historic smoke scenarios show large regional effects on population-weighted smoke exposure across the West. However, the maximum smoke scenarios indicate that smoke exposures would have been even larger in some receptors if the November 2018 and September 2020 wildfires had occurred in different months during the same fire season. The bottom row of Figure 2 presents the “maximum smoke” population-weighted exposure for each receptor for the 2018 and 2020 fire seasons. This scenario, as described above, assumes fixed emissions (November 2018 or September 2020) for all months in each season, but monthly varying meteorology.

In 2018 in the maximum smoke scenario, most state receptors except for NorCal and WA/OR experience slightly higher smoke $\text{PM}_{2.5}$ exposure in the months preceding November 2018. This difference is driven by the combination of factors occurring earlier in the season: faster advection, which carries the smoke from source regions, and drier conditions, which lengthen the lifetime of smoke $\text{PM}_{2.5}$ in the atmosphere. The average horizontal windspeed in the West excluding the coastal states is higher in August and September compared to the months immediately before and after (Figure S2), while average total convective precipitation in August (0.002 mm/day) and September (0.001 mm/day) is less than that in October (0.004 mm/day). Although November has the highest average horizontal windspeeds in the interior West, greater local rainfall earlier in October combined with the relatively smaller fuel load in the interior compared to coastal states lead to lower smoke exposures. The mean West adjoint sensitivities reflect these conditions, with the lowest values occurring earlier in the season (July: 3399, August: 3243, September: 3214, October: 3806 $\text{mg m}^{-3}/\text{g m}^{-2} \text{ s}^{-1}$), implying less transport of smoke from source regions compared to that in November, when the mean adjoint sensitivity is 4366 $\text{mg m}^{-3}/\text{g m}^{-2} \text{ s}^{-1}$. We find that smoke $\text{PM}_{2.5}$ from NorCal dominated emissions during the 2018 fire season, with the exposures at all other receptors are quite small, under $3 \mu\text{g}/\text{m}^3$. Thus, we can conclude that November 2018 leads to the highest possible smoke $\text{PM}_{2.5}$ exposures in NorCal due to its large population and relatively stagnant conditions during that time. The influence of NorCal is also evident in the domain-wide smoke exposure (Figure S4).

In 2020, a different story emerges in the “maximum smoke” scenarios. All receptors except for WA/OR experience higher smoke $\text{PM}_{2.5}$ outside the month of September, especially later in the season. For ID/UT and NV (often together referred to as the “Great Basin”), smoke exposures are $\sim 5 \mu\text{g}/\text{m}^3$ higher when the maximum emissions burn in July and August 2020, instead of September. In October and November, NorCal and the CVCa experience smoke $\text{PM}_{2.5}$ concentrations of 147 and 200 $\mu\text{g}/\text{m}^3$, respectively, which exceed the 87 and 128 $\mu\text{g}/\text{m}^3$ exposures these receptors experience respectively in September. This large disparity in potential smoke exposure is again driven by the greater stagnation occurring later in the fire season. In October and November, average horizontal windspeeds in NorCal are lower than in previous months (Figure S1), which may be due to weakening of the “Diablo Winds” in the CVCa region (Liu et al., 2021). The mean West adjoint sensitivities in the 2020 fire season peak in October (3517 $\text{mg m}^{-3}/\text{g m}^{-2} \text{ s}^{-1}$) rather than September (3339 $\text{mg m}^{-3}/\text{g m}^{-2} \text{ s}^{-1}$) or the other months (July: 2489, August: 2894, November: 3348 $\text{mg m}^{-3}/\text{g m}^{-2} \text{ s}^{-1}$). Finally, although the NavN experiences smoke exposures of only $\sim 5 \mu\text{g}/\text{m}^3$ if the 2020 fires occur in October 2020, these tribal lands generally have a $\text{PM}_{2.5}$ background of $\sim 5 \mu\text{g}/\text{m}^3$, suggesting a doubling of $\text{PM}_{2.5}$ exposure largely from wildfires located hundreds of miles away on the West Coast.

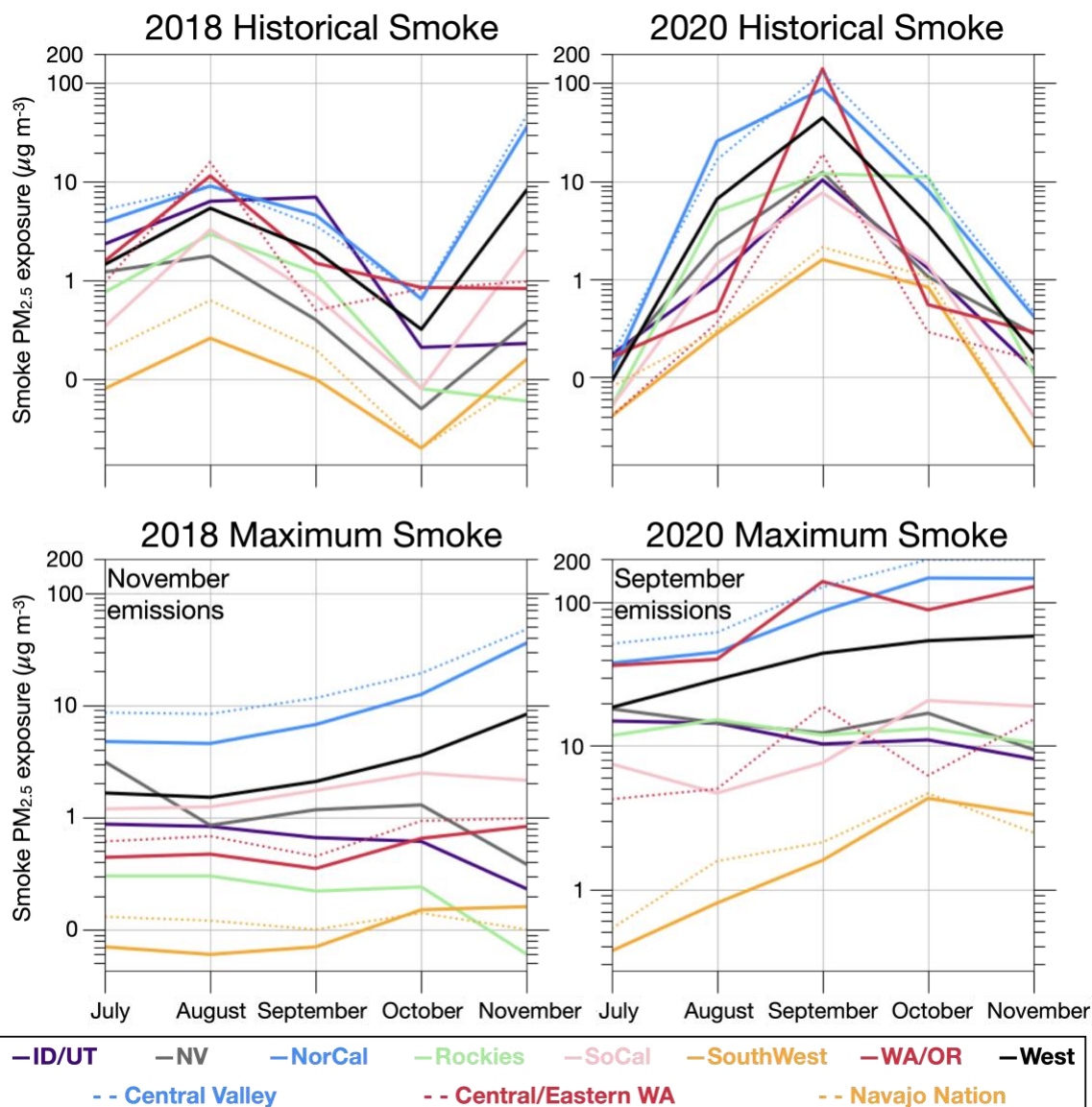


Figure 2. Population-weighted smoke $PM_{2.5}$ exposure for states and rural environmental justice communities in the West for the 2018 and 2020 fire seasons. The concentrations of smoke $PM_{2.5}$ are plotted on a log scale, with the minor axis tick marks delineating the intervals between decades. The top row shows exposures in the historical smoke scenarios, in which monthly mean fire emissions in the 2018 and 2020 fire seasons are multiplied by their paired monthly adjoint sensitivity. The bottom row shows the exposures in the maximum smoke scenarios, in which the largest monthly-mean fire emissions are fixed for each year (November 2018 and September 2020) and are multiplied by each monthly map of adjoint sensitivities. The rural environmental justice communities are represented by dashed lines with the same color as the state receptor that is closest to them spatially. The black line ("West") represents population-weighted smoke exposure across the entire western United States. All smoke exposure values in the figure are found in the Supporting Information.

We find that wildfires in the coastal states contribute more to overall smoke exposure in the West compared to wildfires in other states in both 2018 and 2020 (Figures S7 and 3, center panels).

The largest drivers of this outsized influence of West Coast fires on population-weighted smoke exposure include: (1) prevailing westerly winds, (2) large population centers along the coast, and (3) denser fuel loads west of the Sierra Nevada and Cascade Mountain Ranges, which generate greater smoke emissions when burned. The maximum smoke scenarios for fires in other years generally support this hypothesis. All the significant fire events outside of the 2018 and 2020 fire seasons (Section 2.1) yield population-weighted smoke exposures of less than $5 \mu\text{g}/\text{m}^3$ at our 11 receptors (Figure S5, S6). The Murphy Complex Fire and the Milford Flat Fire cause the highest exposures at the ID/UT receptor, in which the fires originated, across all adjoint sensitivity months, although NorCal and WA/OR are comparable in October and November of the 2018 and 2020 fire seasons. The Wallow fire in Arizona increases local smoke exposure in the SouthWest by as much as $4 \mu\text{g}/\text{m}^3$ but has little impact on any other receptor, with the entire West experiencing less than $1 \mu\text{g}/\text{m}^3$ of smoke. The Whitewater-Baldy complex Fire in New Mexico has little effect in the SouthWest and other receptors due to relatively low fuel load and correspondingly small emissions. However, fires in Colorado during this month lead to higher smoke exposures in the Rockies at around $3 \mu\text{g}/\text{m}^3$. Finally, the Lodgepole Complex Fire in Montana leads to the largest smoke exposures in WA/OR, CEWash, NorCal, and CVCal, rather than locally in the Rockies. We attribute this discrepancy due to the fires located near the Montana-Idaho state line, with relatively larger populations in WA/OR and NorCal yielding higher population-weighted smoke exposure.

These high-fire case studies reveal that though significant smoke emissions can occur outside of the West Coast, these emissions tend to have little impact on smoke exposure on the West as a whole ($<1 \mu\text{g}/\text{m}^3$). We acknowledge that using adjoint weather sensitivities from only the 2018 and 2020 fire seasons may dampen or bias the calculated exposures from these fires. Nonetheless we generally find that the fires in other years emit less smoke than those in NorCal and WA/OR and consequently have a smaller exposure impact. Accordingly, in the next section we will focus our prescribed fire scenario with emissions from only the 2018 and 2020 fire seasons.

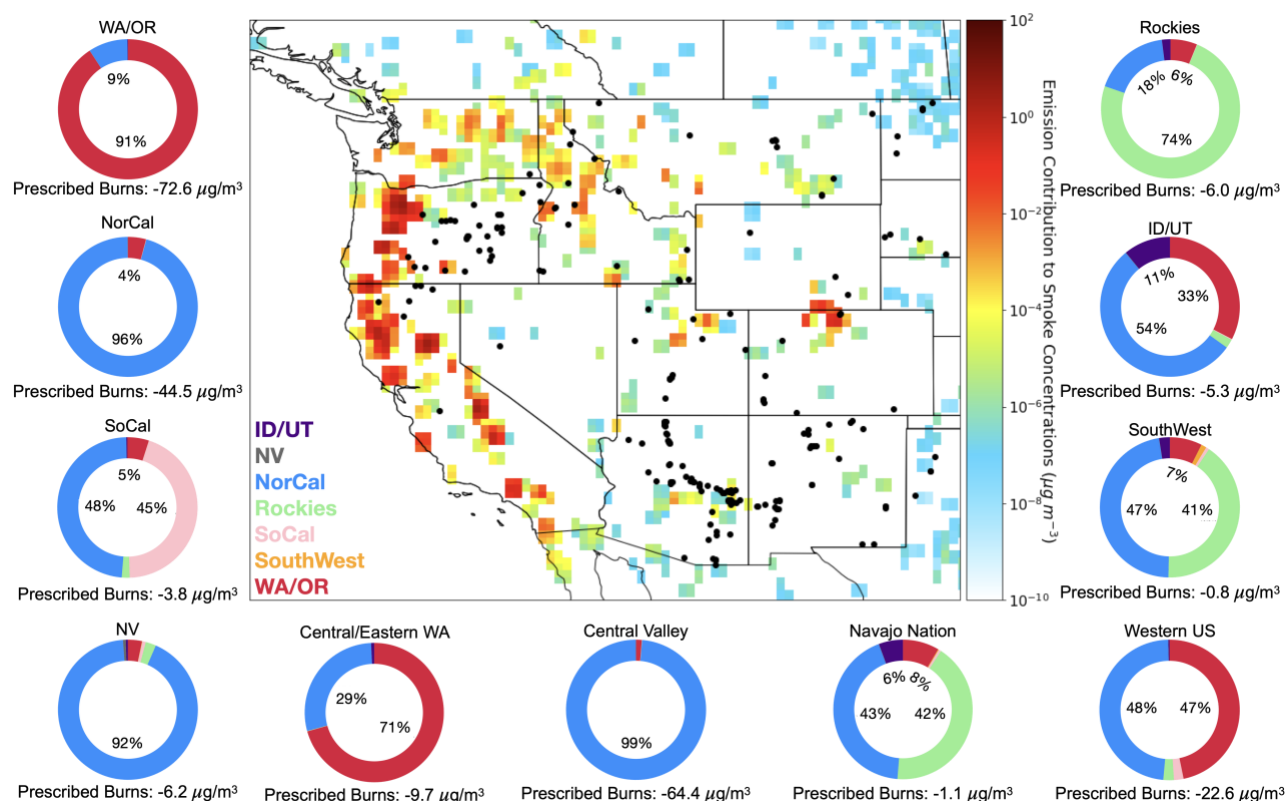


Figure 3. Contributions to population-weighted smoke exposure for the western United States in September 2020 (center panel) and effects of applying prescribed burning interventions in all receptors in the West during this month (pie charts). The center panel shows the locations of MTBS prescribed burn (>1000 acres) during 2015-2020 (black dots, n=190) and the contribution of smoke PM_{2.5} emissions in each grid cell to population-weighted smoke exposure in the West receptor (colors). These contributions are calculated through multiplication of the GEOS-Chem adjoint sensitivities [$\text{mg m}^{-3}/\text{g m}^{-2} \text{s}^{-1}$] of the West population-weighted receptor by the GFED fire emissions [$\text{g m}^{-2} \text{s}^{-1}$] for the month of September 2020. The pie charts in the side panels illustrate the contribution to that smoke reduction from the application of prescribed burns in each receptor, with the values inset indicating the overall reduction of smoke exposure from prescribed burning interventions within that receptor. For example, prescribed burning interventions in WA/OR (upper left) would reduce population-weighted smoke exposure in that receptor by 72.6 $\mu\text{g}/\text{m}^3$ in September 2020 with 91% of that reduction from local prescribed burns in-state and 9% from out-of-state prescribed burns in NorCal.

3.2 Efficacy of prescribed burning locally and across the West

We now investigate the efficacy of prescribed fires as a policy intervention for states in the western United States. Figure 3 (side panels) shows the effect of applying the prescribed burning scenarios within each receptor and their effects on the population-weighted smoke exposure locally and on all other receptors for September 2020. In September 2020, most wildfire smoke emanates from the West Coast. With application of prescribed burning in the NorCal receptor as described in Section 2.4, local smoke exposure decreases by $43 \mu\text{g}/\text{m}^3$ and smoke exposures in all other receptors declines by 40% or more except in WA/OR, CEWash, and the Rockies. An additional reduction of $1.5 \mu\text{g}/\text{m}^3$ of smoke occurs in NorCal with prescribed burns in WA/OR. The prescribed burning interventions in WA/OR further cuts local smoke exposure by $66 \mu\text{g}/\text{m}^3$ and reduces smoke in ID/UT by 33%. Outside of NorCal and WA/OR, the Rockies is the only other region in which application of the prescribed burn scenario within the region reduces local smoke exposure by 50% or more. Finally, we find that prescribed burns applied only in NorCal and WA/OR decreases the population-weighted smoke exposure across the entire West by $21 \mu\text{g}/\text{m}^3$ in September 2020. A similar analysis for November 2018 yields the same conclusion that NorCal and WA/OR control the burden of smoke exposure in the western United States (Figure S7). If the same prescribed fire scenario emissions are multiplied against adjoint sensitivities from different months in each fire season, we would expect similar results with little variance.

We further find that rural environmental justice communities also benefit from prescribed burns in NorCal and WA/OR. In the historical scenario, the CVCal experiences a monthly mean smoke exposure of $128 \mu\text{g}/\text{m}^3$ in September 2020; this exposure is nearly eliminated by the prescribed burn scenario within the NorCal region. Similarly, smoke exposure in CEWash is reduced by $\sim 10 \mu\text{g}/\text{m}^3$ by the prescribed burns in NorCal and WA/OR. In the historical scenario, the NavN in the desert SouthWest experiences over half of its smoke exposure from fires along the West Coast. Although prescribed burns reduce smoke $\text{PM}_{2.5}$ by only $\sim 1 \mu\text{g}/\text{m}^3$ for the Navajo population, studies demonstrate that such incremental decreases in $\text{PM}_{2.5}$ in relatively clean air may still bring a larger than expected benefit to public health (Feng et al., 2016; Shi et al., 2016).

Taken together, these results suggest that implementing prescribed burns in NorCal and WA/OR would yield large net benefits for the entire western United States, while doing so in other states would have relatively smaller impacts. In addition, the mean adjoint sensitivities for the 2018 and 2020 fire seasons suggest that prescribed burning interventions should occur before the fire season in the spring when the meteorological potential (e.g., stagnation, dry weather, or strong, dispersive winds) to drive smoke exposure is lower. To an extent, such practices are already being implemented in the Southwestern United States where prescribed burns are increasingly conducted in the spring when: (1) wind speeds are relatively weaker, (2) many of the heavier surface fuels are still somewhat moist from the winter, and (3) precipitation is greater (US Department of Agriculture Forest Service, 2009).

Our modeling results in tandem with the historical record suggest that large, prescribed burns may help limit smoke exposure in subsequent years but that such burns are not occurring in key areas. The central panel of Figure 3 presents the MTBS locations of large, prescribed burns over the course of 2015-2020 ($n=190$), plotted against the contribution of fire emissions in each grid cell to the population-weighted smoke exposure for the whole of the western United States for

September 2020. As expected, the largest contributions occur in NorCal, western Oregon, eastern Washington, with hotspots in Idaho and the Front Range in Colorado. These areas agree well with our diagnosis of those locations that control smoke exposure in the West. Nearly half of the 2015-2020 large, prescribed burns occurred in Arizona (n=58, Gila National Forest) and Central Oregon (n=31, agricultural burning) (Figure S8), regions which subsequently experienced little fire in 2020. In contrast, fewer than 10 large, prescribed burns occurred during this timeframe in NorCal and western Oregon, areas that our work shows have a disproportionate impact on smoke exposure for rural environmental justice communities and as well as population centers across the West. These MTBS prescribed fires primarily occurred on federal lands (Y. Li et al., 2020), except in central Oregon which is dominated by agricultural burning. Fuel load and meteorology are significant drivers of this West Coast smoke exposure relationship because west of the Sierras/Cascades rain is more abundant, vegetation is woodier, and the region thus generates more smoke emissions. On the other hand, in the rain shadow east of the Sierras/Cascades, precipitation tends to be lower and vegetation scrubrier, leading to less smoke emissions.

Our work suggests that NorCal may benefit from applying a small number of large, prescribed burns instead of many small, prescribed burns. We find that the annual burned area from prescribed fires in NorCal are less than 11% (Table S1) of fire burned area in all of California before human intervention as hypothesized in one study that took into account fire return intervals for different vegetation types (Stephens et al., 2007). This comparison, a measure of the fire deficit, is of value since most wildfire area burned in California occurs in the NorCal receptor. NFPORS indicates that NorCal applied 9,590 prescribed burns over the course of 2018-2020, yet only 88 (0.9%) of these burns were larger than 500 acres (~2 sq. km) (Figure 4). We find that the NFPORS records of prescribed fires larger than 1000 acres agree well with MTBS, which exclusively reports prescribed fires larger than 1000 acres. Our findings in Central Oregon and in Arizona imply that large, prescribed burns greater than 1000 acres in NorCal may have the potential to limit smoke exposure from wildfires across the West. NorCal is a populous and mountainous region with dense and woody fuel load, which requires significant firefighting resources to manage even small, prescribed burns. Although the societal sensitivity to smoke is acutely heightened in the West (Kolden, 2019), wildland fire managers may consider applying an optimal number of large, prescribed burns to minimize air pollution exposure given limited resources.

More work is needed to confirm the long-term effects of prescribed burning, but our results suggest that the limited number of prescribed burns in key regions such as NorCal may be effective in reducing the impacts of smoke on the West.

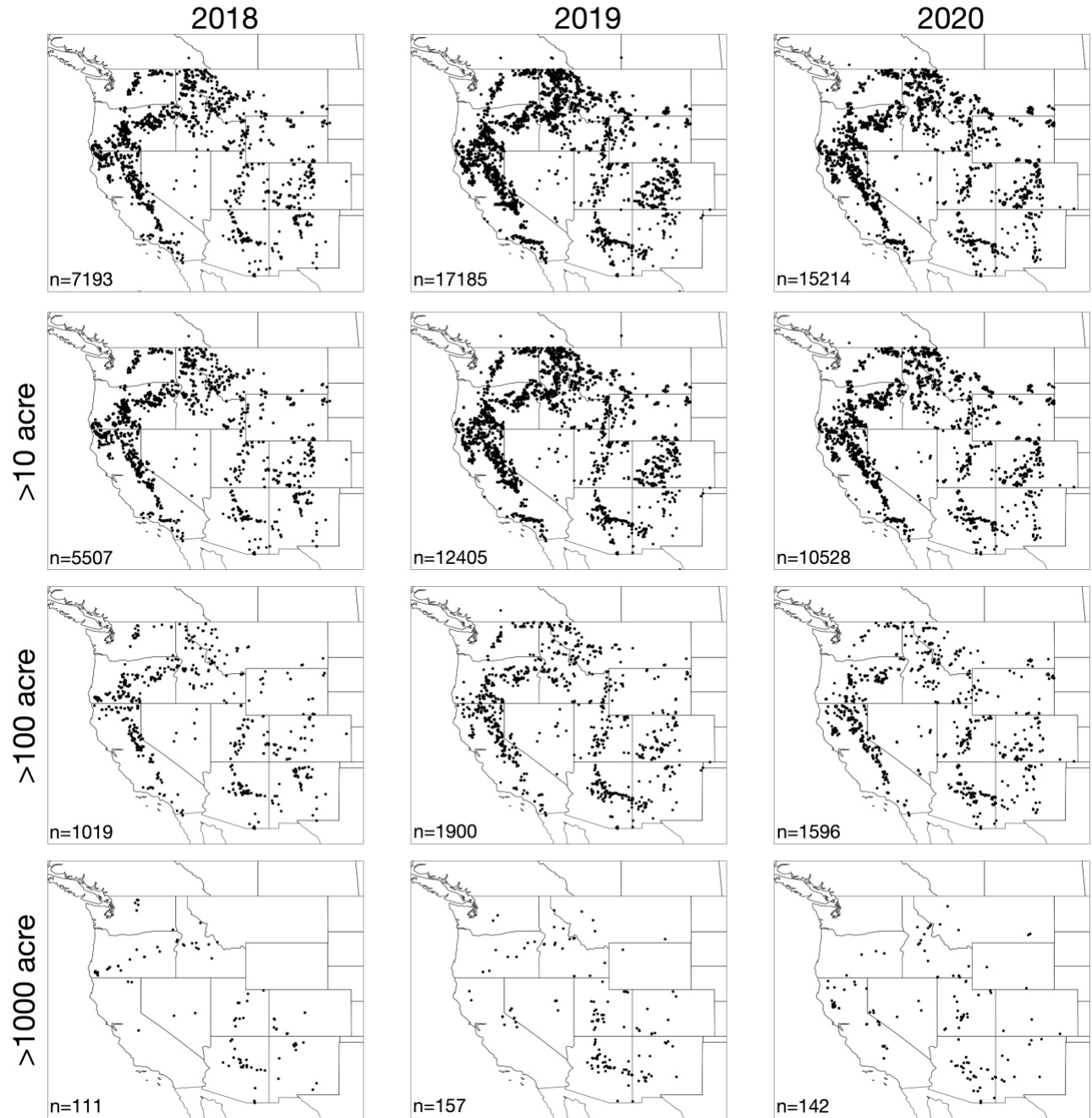


Figure 4. NFPORS historical record of prescribed fires filtered by acres burned over 2018-2020. The figure shows the location of NFPORS-reported prescribed burn locations (black dots). The first row shows all prescribed burns in the database with each subsequent row removing prescribed fires smaller than 10, 100, and 1000 acres. The inset of each figure reports the total number of prescribed burns during that year given the filtering condition. Table S1 reports the prescribed fire total burned acreage and number of fires over the course of 2018 to 2020 in the NorCal receptor.

Conclusions:

This work explores the efficacy of prescribed burning as a land management intervention for mitigating smoke exposure in population centers and rural environmental justice communities downwind of potential wildfires across the western United States. The motivation stems from the relative lack of prescribed burning studies on the impacts of smoke exposure abatement.

Our study integrates information on the drivers of fire emissions in the western United States, the transport of smoke to downwind receptors, and the resulting population exposure to wildfire smoke. While earlier studies using a similar framework investigated air pollution in Southeast Asia, here we do so for the western United States. Our study characterizes how meteorological variability modulates smoke exposure and quantifies the efficacy of prescribed burning as a land management tool in the western United States. We acknowledge that prescribed burning worsens air quality in specific locations on short-term time scales, although we demonstrate here that it has the capability to reduce state and community smoke exposure, in some cases dramatically. Our method employs the GEOS-Chem adjoint model to calculate the sensitivities of population-weighted smoke $\text{PM}_{2.5}$ concentrations in specified regions to fire emissions and their spatiotemporal distributions during the 2018 and 2020 fire seasons.

We show that the West Coast both experiences the largest population-weighted smoke exposures and contributes most to the burden of smoke $\text{PM}_{2.5}$ in the western United States. For the high of each fire season (November 2018 and September 2020), the coastal states accounted for 95% of the burden of population smoke exposure across the West (Figure 3 and S7). In 2018, the Camp Fire in Northern California caused a monthly-mean increase of $8.3 \mu\text{g}/\text{m}^3$ of population smoke exposure in the western United States. In September 2020, the West Coast experienced monthly average smoke concentrations of $140 \mu\text{g}/\text{m}^3$ in Washington and Oregon, and $87 \mu\text{g}/\text{m}^3$ in Northern California while all other states' smoke exposure was under $13 \mu\text{g}/\text{m}^3$. Although the examination of high-fire cases outside of the coastal states reveals significant smoke emissions, these emissions tend to have little impact on smoke exposure on the West as a whole ($<1 \mu\text{g}/\text{m}^3$). We also demonstrate that northern California, western Oregon, and eastern Washington are areas that have a disproportionate impact on smoke exposure for rural environmental justice communities and as well as population centers across the West. The largest drivers of this outsized influence of West Coast fires on population-weighted smoke exposure include: (1) prevailing westerly winds, (2) large population centers along the coast, and (3) denser fuel loads west of the Sierra Nevada and Cascade Mountain Ranges which generate greater smoke emissions when burned.

We also create “maximum smoke” exposure scenarios in which monthly mean emissions are fixed to the high of each fire season while meteorology is allowed to vary. We find that the largest population-weighted smoke exposures in 2018 did in fact occur in November due to large-scale regional stagnation over northern California during that time of year, whereas in 2020, smoke exposures would have been even greater if the wildfires had occurred in October or November. The average adjoint sensitivities for northern California, which can be used to infer the relative importance of meteorology vs. emissions in driving smoke exposures, corroborates this result with November 2018 yielding nearly double the levels of meteorological influence (here, stagnation) compared to other months in the fire season.

Our results suggest that prescribed burns may reduce the smoke impacts from future large wildfires in the West but that few such burns have occurred in northern California and western Oregon. We find that widespread prescribed burning interventions across northern California and the Pacific Northwest could have reduced the population smoke exposure of the entire western United States by $21 \mu\text{g}/\text{m}^3$ in September 2020, while doing so in other states would have reduced smoke exposure by only $1.5 \mu\text{g}/\text{m}^3$. The mean adjoint sensitivities for the 2018 and 2020 fire seasons suggest that possible prescribed burning interventions should occur earlier in the fire season or even before the season begins, when chances of meteorological influence (e.g., stagnation or strong, dispersive winds) are lower, and the fuel load is still moist from spring precipitation. Furthermore, we find that the large, prescribed fires applied from 2015-2020 in Arizona ($n=58$) and Central Oregon ($n=31$) may have led to fewer fires in 2020, which in turn suggests that prescribed burns may help reduce fuel load in future large wildfires. However, northern California and western Oregon conducted only seven prescribed fires greater than 1000 acres in area over a 6-year period (2015-2020). Given that this region is largely responsible for the burden of smoke $\text{PM}_{2.5}$ exposure in the western United States, our analysis recommends prioritizing northern California and the Pacific Northwest as areas for future prescribed burning research.

States in the West may benefit from applying a small number of large, prescribed burns instead of many small, prescribed burns. We find that the annual burned area from prescribed fires in Northern California is less than 11% (Table S1) of one estimate of fire burned area pre-European intervention (Stephens et al., 2007). NFORS indicates that Northern California applied 9,590 prescribed burns over the course of 2018-2020, yet only 88 (0.9%) of these burns were larger than 500 acres ($\sim 2 \text{ sq. km}$) (Figure 4). NorCal is a populous and mountainous region with dense and woody fuel load, which requires significant firefighting resources to manage even small, prescribed burns. As these large, complex, and costly wildfires become more common, innovative methods to identify locations for prescribed burning are needed to mitigate impacts on affected populations and ecosystems. Wildland fire managers may consider applying an optimal number of large, prescribed burns to minimize air pollution exposure given limited resources.

The rural dimensions of environmental justice studies have long been present (Pellow, 2016), but the recent developments of high-resolution air pollution datasets largely have shifted the focus of such studies to urban centers. For example, many of the early environmental justice movement battlegrounds in the United States took place in rural communities like Warren County, North Carolina (McGurty, 2000), but few recent studies analyze the conditions of such communities with regard to air pollution and smoke exposure from fires. Our work aims to add to the environmental justice literature for rural communities in the Central Valley in California, Central/Eastern Washington State, and the Navajo Native American reservation. We model the transport of smoke to these regions from recent wildfires in the West, quantify the population-weighted exposures, and discuss the susceptibility of these vulnerable communities.

We acknowledge several limitations in the spatiotemporal scope of our work. We simulated only the adjoint sensitivities for the 2018 and 2020 fire seasons (July-November) and assumed that these meteorological fields account for most of the weather variability that may occur in a fire season. These sensitivities may not be applicable under new climate extremes. In addition, we

used monthly fire emissions and adjoint sensitivity simulations which may not capture daily smoke $\text{PM}_{2.5}$ extremes. Similarly, the $0.25^\circ \times 0.3125^\circ$ (roughly 25 km^2) horizontal resolution of the GEOS-Chem adjoint simulations and the relatively large size of our receptors are useful for quantifying the distribution of smoke at a regional scale but may be too coarse for analyzing fires at a neighborhood scale. The MTBS historical records of prescribed burn locations only account for prescribed fires that burned over 1000 acres ($\sim 4 \text{ km}^2$) and do not include smaller fires. The NFPORS historical records of prescribed burning does not report pile burning which may constitute a significant fraction of small (< 1000 acres), prescribed fires.

Smoke from wildfires represents a significant human health and ecosystem hazard. With the frequency and magnitude of such fires predicted to increase further into the future (Duffy et al., 2019) and with a growing scarcity of fire-fighting resources (Belval et al., 2020), identifying where to carry out prescribed fires is becoming especially important. Land management personnel in the United States typically do not take into account averted smoke exposure from wildfires when planning prescribed fires, though air pollution is the largest environmental cause of mortality worldwide and wildfire smoke is the largest contributor to poor air quality in the West. Our work helps determine where the application of prescribed fires would yield the greatest net benefit for states and environmental justice communities, in terms of minimizing population smoke exposure. We posit that our study may help stakeholders and land managers weigh the benefits and hazards of prescribed fires.

Acknowledgements and Data

This study was supported by the NOAA Climate Program Office's Modeling, Analysis, Predictions, and Projections Program (MAPP), Grant NA22OAR4310140. The authors wish to thank Zichong Chen and Zhen Qu for GEOS-Chem adjoint advice, Yurika Harada for her contribution to GIS visualization, and Dana Skelly for access to the NFPORS database.

Data Availability Statement

Code and supporting material for the GEOS-Chem Adjoint model used in this work can be found at Zenodo (<https://zenodo.org/record/7517355>).

REFERENCES

- Abatzoglou, J.T., Rupp, D.E., O'Neill, L.W., Sadegh, M., 2021. Compound Extremes Drive the Western Oregon Wildfires of September 2020. *Geophysical Research Letters* 48, e2021GL092520. <https://doi.org/10.1029/2021GL092520>
- Abatzoglou, J.T., Williams, A.P., 2016. Impact of anthropogenic climate change on wildfire across western US forests. *PNAS* 113, 11770–11775. <https://doi.org/10.1073/pnas.1607171113>
- Baker, K.; Rao, V.; Beidler, J.; Vukovich, J.; Koplitz, S.; Avey, L., 2020. Illustrating wildland fire air quality impacts using an EPA emission inventory [Magazine]. *EM: Environmental Manager*, 24, 26-31.
- Balch, J.K., Bradley, B.A., Abatzoglou, J.T., Nagy, R.C., Fusco, E.J., Mahood, A.L., 2017. Human-started wildfires expand the fire niche across the United States. *Proceedings of the National Academy of Sciences* 114, 2946–2951. <https://doi.org/10.1073/pnas.1617394114>
- Barbero, R., Abatzoglou, J.T., Steel, E.A., Larkin, N.K., 2014. Modeling very large-fire occurrences over the continental United States from weather and climate forcing. *Environ. Res. Lett.* 9, 124009. <https://doi.org/10.1088/1748-9326/9/12/124009>
- Bay City News, 2018. Wildland Development Escalates California Fire Costs. KQED, <https://www.kqed.org/news/11713393/wildland-development-escalates-california-fire-costs>.
- Belval, E.J., Stonesifer, C.S., Calkin, D.E., 2020. Fire Suppression Resource Scarcity: Current Metrics and Future Performance Indicators. *Forests* 11, 217. <https://doi.org/10.3390/f11020217>
- Bey, I., Jacob, D.J., Yantosca, R.M., Logan, J.A., Field, B.D., Fiore, A.M., Li, Q., Liu, H.Y., Mickley, L.J., Schultz, M.G., 2001. Global modeling of tropospheric chemistry with assimilated meteorology: Model description and evaluation. *Journal of Geophysical Research: Atmospheres* 106, 23073–23095. <https://doi.org/10.1029/2001JD000807>
- Bi, J., Carmona, N., Blanco, M.N., Gassett, A.J., Seto, E., Szpiro, A.A., Larson, T.V., Sampson, P.D., Kaufman, J.D., Sheppard, L., 2022. Publicly available low-cost sensor measurements for PM_{2.5} exposure modeling: Guidance for monitor deployment and data selection. *Environment International* 158, 106897. <https://doi.org/10.1016/j.envint.2021.106897>
- Bindle, L., Martin, R.V., Cooper, M.J., Lundgren, E.W., Eastham, S.D., Auer, B.M., Clune, T.L., Weng, H., Lin, J., Murray, L.T., Meng, J., Keller, C.A., Putman, W.M., Pawson, S., Jacob, D.J., 2021. Grid-stretching capability for the GEOS-Chem 13.0.0 atmospheric chemistry model. *Geoscientific Model Development* 14, 5977–5997. <https://doi.org/10.5194/gmd-14-5977-2021>
- Brewer, M.J., Clements, C.B., 2020. The 2018 Camp Fire: Meteorological Analysis Using In Situ Observations and Numerical Simulations. *Atmosphere* 11, 47. <https://doi.org/10.3390/atmos11010047>
- California Air Resources Board, 2021. Camp Fire Air Quality Data Analysis. https://ww2.arb.ca.gov/sites/default/files/2021-07/Camp_Fire_report_July2021.pdf
- Cedar River Group, 2012. On Common Ground: Meeting The Need For Farmworker Housing in Washington State. https://cedarrivergroup.com/crgwpf/wp-content/uploads/2013/12/On-Common-Ground_-_Need-for-Farmworker-Housing-in-Washington-ver-1212121.pdf

- Chandrasekaran, P.R., 2021. Remaking “the people”: Immigrant farmworkers, environmental justice and the rise of environmental populism in California’s San Joaquin Valley. *Journal of Rural Studies* 82, 595–605. <https://doi.org/10.1016/j.jrurstud.2020.08.043>
- Childs, M.L., Li, J., Wen, J., Heft-Neal, S., Driscoll, A., Wang, S., Gould, C.F., Qiu, M., Burney, J., Burke, M., 2022. Daily Local-Level Estimates of Ambient Wildfire Smoke PM_{2.5} for the Contiguous US. *Environ. Sci. Technol.* <https://doi.org/10.1021/acs.est.2c02934>
- CIESIN, 2018. Gridded Population of the World, Version 4 (GPWv4): Population Density Adjusted to Match 2020 Revision UN WPP Country Totals, Revision 11. Palisades, NY.
- Colorado Division of Fire Prevention and Control, 2022. Colorado's Largest Fires by Acreage. <https://dfpc.colorado.gov/wildfire-information-center/historical-wildfire-information>
- Davies, I.P., Haugo, R.D., Robertson, J.C., Levin, P.S., 2018. The unequal vulnerability of communities of color to wildfire. *PLOS ONE* 13, e0205825. <https://doi.org/10.1371/journal.pone.0205825>
- deSouza, P., Kinney, P.L., 2021. On the distribution of low-cost PM_{2.5} sensors in the US: demographic and air quality associations. *J Expo Sci Environ Epidemiol* 31, 514–524. <https://doi.org/10.1038/s41370-021-00328-2>
- Di, Q., Amini, H., Shi, L., Kloog, I., Silvern, R., Kelly, J., Sabath, M.B., Choirat, C., Koutrakis, P., Lyapustin, A., Wang, Y., Mickley, L.J., Schwartz, J., 2019. An ensemble-based model of PM_{2.5} concentration across the contiguous United States with high spatiotemporal resolution. *Environment International* 130, 104909. <https://doi.org/10.1016/j.envint.2019.104909>
- Duffy, P.B., Field, C.B., Diffenbaugh, N.S., Doney, S.C., Dutton, Z., Goodman, S., Heinzerling, L., Hsiang, S., Lobell, D.B., Mickley, L.J., Myers, S., Natali, S.M., Parmesan, C., Tierney, S., Williams, A.P., 2019. Strengthened scientific support for the Endangerment Finding for atmospheric greenhouse gases. *Science* 363, eaat5982. <https://doi.org/10.1126/science.aat5982>
- Eastham, S.D., Long, M.S., Keller, C.A., Lundgren, E., Yantosca, R.M., Zhuang, J., Li, C., Lee, C.J., Yannetti, M., Auer, B.M., Clune, T.L., Kouatchou, J., Putman, W.M., Thompson, M.A., Trayanov, A.L., Molod, A.M., Martin, R.V., Jacob, D.J., 2018. GEOS-Chem High Performance (GCHP v11-02c): a next-generation implementation of the GEOS-Chem chemical transport model for massively parallel applications. *Geoscientific Model Development* 11, 2941–2953. <https://doi.org/10.5194/gmd-11-2941-2018>
- Feng, S., Gao, D., Liao, F., Zhou, F., Wang, X., 2016. The health effects of ambient PM_{2.5} and potential mechanisms. *Ecotoxicology and Environmental Safety* 128, 67–74. <https://doi.org/10.1016/j.ecoenv.2016.01.030>
- Finco, M., Quayle, B., Zhang, Y., Lecker, J., Megown, K.A., Brewer, C.K., 2012. Monitoring Trends and Burn Severity (MTBS): Monitoring wildfire activity for the past quarter century using landsat data. In: Morin, Randall S.; Liknes, Greg C., comps. *Moving from status to trends: Forest Inventory and Analysis (FIA) symposium 2012*; 2012 December 4-6; Baltimore, MD. Gen. Tech. Rep. NRS-P-105. Newtown Square, PA: U.S. Department of Agriculture, Forest Service, Northern Research Station. [CD-ROM]: 222-228.
- Fire and Environmental Research Applications Team (FERA), 2020. Fuel and fire tools. <https://www.fs.usda.gov/pnw/tools/fuel-and-fire-tools-fft>.
- Garcia, J., 2007. *Mexicans in North Central Washington* (San Francisco, CA: Arcadia Publishing)

- Geographic Area Coordination Center, 2020. 2020 National Large Incident Year-to-Date Report. National Interagency Fire Center. December 21, 2020. Archived from the original (PDF) on December 29, 2020.
- Giglio, L., Schroeder, W., Justice, C.O., 2016. The collection 6 MODIS active fire detection algorithm and fire products. *Remote Sensing of Environment* 178, 31–41. <https://doi.org/10.1016/j.rse.2016.02.054>
- Griffin, D., McLinden, C.A., Dammers, E., Adams, C., Stockwell, C.E., Warneke, C., Bourgeois, I., Peischl, J., Ryerson, T.B., Zarzana, K.J., Rowe, J.P., Volkamer, R., Knote, C., Kille, N., Koenig, T.K., Lee, C.F., Rollins, D., Rickly, P.S., Chen, J., Fehr, L., Bourassa, A., Degenstein, D., Hayden, K., Mihele, C., Wren, S.N., Liggio, J., Akingunola, A., Makar, P., 2021. Biomass burning nitrogen dioxide emissions derived from space with TROPOMI: methodology and validation. *Atmospheric Measurement Techniques* 14, 7929–7957. <https://doi.org/10.5194/amt-14-7929-2021>
- Guiterman, C.H., Margolis, E.Q., Baisan, C.H., Falk, D.A., Allen, C.D., Swetnam, T.W., 2019. Spatiotemporal variability of human–fire interactions on the Navajo Nation. *Ecosphere* 10, e02932. <https://doi.org/10.1002/ecs2.2932>
- Hantson, S., Andela, N., Goulden, M.L., Randerson, J.T., 2022. Human-ignited fires result in more extreme fire behavior and ecosystem impacts. *Nat Commun* 13, 2717. <https://doi.org/10.1038/s41467-022-30030-2>
- Henze, D.K., Hakami, A., Seinfeld, J.H., 2007. Development of the adjoint of GEOS-Chem. *Atmospheric Chemistry and Physics* 7, 2413–2433. <https://doi.org/10.5194/acp-7-2413-2007>
- H.R.5376 - 117th Congress (2021-2022): Inflation Reduction Act of 2022. (2022, August 16). <http://www.congress.gov/>
- Jaffe, D.A., O'Neill, S.M., Larkin, N.K., Holder, A.L., Peterson, D.L., Halofsky, J.E., Rappold, A.G., 2020. Wildfire and prescribed burning impacts on air quality in the United States. *Journal of the Air & Waste Management Association* 70, 583–615. <https://doi.org/10.1080/10962247.2020.1749731>
- Jbaily, A., Zhou, X., Liu, J., Lee, T.-H., Kamareddine, L., Verguet, S., Dominici, F., 2022. Air pollution exposure disparities across US population and income groups. *Nature* 601, 228–233. <https://doi.org/10.1038/s41586-021-04190-y>
- Kelp, M.M., Lin, S., Kutz, J.N., Mickley, L.J., 2022. A new approach for determining optimal placement of PM_{2.5} air quality sensors: case study for the contiguous United States. *Environ. Res. Lett.* 17, 034034. <https://doi.org/10.1088/1748-9326/ac548f>
- Kim, J., Jeong, U., Ahn, M.H., Kim, J.H., Park, R.J., Lee, Hanlim, Song, C.H., Choi, Y.S., Lee, K.H., Yoo, J.M., Jeong, M.J., Park, S.K., Lee, K.M., Song, C.K., Kim, Sang Woo, Kim, Y.J., Kim, Si Wan, Kim, M., Go, S., Liu, X., Chance, K., Miller, C.C., Al-Saadi, J., Veihermann, B., Bhartia, P.K., Torres, O., Abad, G.G., Haffner, D.P., Ko, D.H., Lee, S.H., Woo, J.H., Chong, H., Park, S.S., Nicks, D., Choi, W.J., Moon, K.J., Cho, A., Yoon, J., Kim, S. kyun, Hong, H., Lee, K., Lee, Hana, Lee, S., Choi, M., Veeffkind, P., Levelt, P.F., Edwards, D.P., Kang, M., Eo, M., Bak, J., Baek, K., Kwon, H.A., Yang, J., Park, J., Han, K.M., Kim, B.R., Shin, H.W., Choi, H., Lee, E., Chong, J., Cha, Y., Koo, J.H., Irie, H., Hayashida, S., Kasai, Y., Kanaya, Y., Liu, C., Lin, J., Crawford, J.H., Carmichael, G.R., Newchurch, M.J., Lefer, B.L., Herman, J.R., Swap, R.J., Lau, A.K.H., Kurosu, T.P., Jaross, G., Ahlers, B., Dobber, M., McElroy, C.T., Choi, Y., 2020. New era

- of air quality monitoring from space: Geostationary environment monitoring spectrometer (GEMS). *Bulletin of the American Meteorological Society* 101, E1–E22. <https://doi.org/10.1175/BAMS-D-18-0013.1>
- Kim, P.S., Jacob, D.J., Mickley, L.J., Kopplitz, S.N., Marlier, M.E., DeFries, R.S., Myers, S.S., Chew, B.N., Mao, Y.H., 2015. Sensitivity of population smoke exposure to fire locations in Equatorial Asia. *Atmospheric Environment* 102, 11–17. <https://doi.org/10.1016/j.atmosenv.2014.09.045>
- Kolden, C.A., 2019. We're Not Doing Enough Prescribed Fire in the Western United States to Mitigate Wildfire Risk. *Fire* 2, 30. <https://doi.org/10.3390/fire2020030>
- Kopplitz, S.N., Mickley, L.J., Marlier, M.E., Buonocore, J.J., Kim, P.S., Liu, T., Sulprizio, M.P., DeFries, R.S., Jacob, D.J., Schwartz, J., Pongsiri, M., Myers, S.S., 2016. Public health impacts of the severe haze in Equatorial Asia in September–October 2015: demonstration of a new framework for informing fire management strategies to reduce downwind smoke exposure. *Environ. Res. Lett.* 11, 094023. <https://doi.org/10.1088/1748-9326/11/9/094023>
- Lake, F.K., Christianson, A.C., 2019. Indigenous fire stewardship. *Encyclopedia of Wildfires and Wildland-Urban Interface (WUI) Fires*. https://doi.org/10.1007/978-3-319-51727-8_225-1
- Lake, F.K., Wright, V., Morgan, P., McFadzen, M., McWethy, D., Stevens-Rumann, C., 2017. Returning Fire to the Land: Celebrating Traditional Knowledge and Fire. *Journal of Forestry* 115, 343–353. <https://doi.org/10.5849/jof.2016-043R2>
- Landguth, E.L., Holden, Z.A., Graham, J., Stark, B., Mokhtari, E.B., Kaleczyc, E., Anderson, S., Urbanski, S., Jolly, M., Semmens, E.O., Warren, D.A., Swanson, A., Stone, E., Noonan, C., 2020. The delayed effect of wildfire season particulate matter on subsequent influenza season in a mountain west region of the USA. *Environment International* 139, 105668. <https://doi.org/10.1016/j.envint.2020.105668>
- Larsen, A.E., Reich, B.J., Ruminski, M., Rappold, A.G., 2018. Impacts of fire smoke plumes on regional air quality, 2006-2013. *J Expo Sci Environ Epidemiol* 28, 319–327. <https://doi.org/10.1038/s41370-017-0013-x>
- Li, L., Girguis, M., Lurmann, F., Pavlovic, N., McClure, C., Franklin, M., Wu, J., Oman, L.D., Breton, C., Gilliland, F., Habre, R., 2020. Ensemble-based deep learning for estimating PM_{2.5} over California with multisource big data including wildfire smoke. *Environment International* 145, 106143. <https://doi.org/10.1016/j.envint.2020.106143>
- Li, Y., Mickley, L.J., Liu, P., Kaplan, J.O., 2020. Trends and spatial shifts in lightning fires and smoke concentrations in response to 21st century climate over the national forests and parks of the western United States. *Atmospheric Chemistry and Physics* 20, 8827–8838. <https://doi.org/10.5194/acp-20-8827-2020>
- Liang, Y., Sengupta, D., Campmeyer, M.J., Lunderberg, D.M., Apte, J.S., Goldstein, A.H., 2021. Wildfire smoke impacts on indoor air quality assessed using crowdsourced data in California. *Proceedings of the National Academy of Sciences* 118, e2106478118. <https://doi.org/10.1073/pnas.2106478118>
- Liu, J.C., Wilson, A., Mickley, L.J., Dominici, F., Ebisu, K., Wang, Y., Sulprizio, M.P., Peng, R.D., Yue, X., Son, J.-Y., Anderson, G.B., Bell, M.L., 2017. Wildfire-specific Fine Particulate Matter and Risk of Hospital Admissions in Urban and Rural Counties. *Epidemiology* 28, 77–85. <https://doi.org/10.1097/EDE.0000000000000556>

- Liu, Y.-C., Di, P., Chen, S.-H., Chen, X., Fan, J., DaMassa, J., Avise, J., 2021. Climatology of diablo winds in Northern California and their relationships with large-scale climate variabilities. *Clim Dyn* 56, 1335–1356. <https://doi.org/10.1007/s00382-020-05535-5>
- Magzamen, S., Gan, R.W., Liu, J., O'Dell, K., Ford, B., Berg, K., Bol, K., Wilson, A., Fischer, E.V., Pierce, J.R., 2021. Differential Cardiopulmonary Health Impacts of Local and Long-Range Transport of Wildfire Smoke. *GeoHealth* 5, e2020GH000330. <https://doi.org/10.1029/2020GH000330>
- Marlier, M.E., Brenner, K.I., Liu, J.C., Mickley, L.J., Raby, S., James, E., Ahmadov, R., Riden, H., 2022. Exposure of agricultural workers in California to wildfire smoke under past and future climate conditions. *Environ. Res. Lett.* 17, 094045. <https://doi.org/10.1088/1748-9326/ac8c58>
- Marlier, M.E., Liu, T., Yu, K., Buonocore, J.J., Koplitz, S.N., DeFries, R.S., Mickley, L.J., Jacob, D.J., Schwartz, J., Wardhana, B.S., Myers, S.S., 2019. Fires, Smoke Exposure, and Public Health: An Integrative Framework to Maximize Health Benefits From Peatland Restoration. *GeoHealth* 3, 178–189. <https://doi.org/10.1029/2019GH000191>
- Marlon, J.R., Bartlein, P.J., Gavin, D.G., Long, C.J., Anderson, R.S., Briles, C.E., Brown, K.J., Colombaroli, D., Hallett, D.J., Power, M.J., Scharf, E.A., Walsh, M.K., 2012. Long-term perspective on wildfires in the western USA. *Proceedings of the National Academy of Sciences* 109, E535–E543. <https://doi.org/10.1073/pnas.1112839109>
- McClure, C.D., Jaffe, D.A., 2018. US particulate matter air quality improves except in wildfire-prone areas. *Proc Natl Acad Sci U S A* 115, 7901–7906. <https://doi.org/10.1073/pnas.1804353115>
- McGurty, E.M., 2000. Warren County, NC, and the Emergence of the Environmental Justice Movement: Unlikely Coalitions and Shared Meanings in Local Collective Action. *Society & Natural Resources* 13, 373–387. <https://doi.org/10.1080/089419200279027>
- Mu, M., Randerson, J.T., van der Werf, G.R., Giglio, L., Kasibhatla, P., Morton, D., Collatz, G.J., DeFries, R.S., Hyer, E.J., Prins, E.M., Griffith, D.W.T., Wunch, D., Toon, G.C., Sherlock, V., Wennberg, P.O., 2011. Daily and 3-hourly variability in global fire emissions and consequences for atmospheric model predictions of carbon monoxide. *Journal of Geophysical Research: Atmospheres* 116. <https://doi.org/10.1029/2011JD016245>
- O'Dell, K., Ford, B., Burkhardt, J., Magzamen, S., Anenberg, S.C., Bayham, J., Fischer, E.V., Pierce, J.R., 2022. Outside in: the relationship between indoor and outdoor particulate air quality during wildfire smoke events in western US cities. *Environ. Res.: Health*. <https://doi.org/10.1088/2752-5309/ac7d69>
- O'Dell, K., Ford, B., Fischer, E.V., Pierce, J.R., 2019. Contribution of Wildland-Fire Smoke to US PM_{2.5} and Its Influence on Recent Trends. *Environ. Sci. Technol.* 53, 1797–1804. <https://doi.org/10.1021/acs.est.8b05430>
- Ospina, M.B., Voaklander, D.C., Stickland, M.K., King, M., Senthilselvan, A., Rowe, B.H., 2012. Prevalence of Asthma and Chronic Obstructive Pulmonary Disease in Aboriginal and Non-Aboriginal Populations: A Systematic Review and Meta-Analysis of Epidemiological Studies. *Canadian Respiratory Journal* 19, 355–360. <https://doi.org/10.1155/2012/825107>
- Pellow, D.N., 2016. Environmental justice and rural studies: A critical conversation and invitation to collaboration. *Journal of Rural Studies* 47, 381–386. <https://doi.org/10.1016/j.jrurstud.2016.06.018>

- Pendergrass, D.C., Zhai, S., Kim, J., Koo, J.-H., Lee, S., Bae, M., Kim, S., Liao, H., Jacob, D.J., 2022. Continuous mapping of fine particulate matter (PM_{2.5}) air quality in East Asia at daily 6 × 6 km² resolution by application of a random forest algorithm to 2011–2019 GOCI geostationary satellite data. *Atmos. Meas. Tech.* 15, 1075–1091. <https://doi.org/10.5194/amt-15-1075-2022>
- Randerson, J.T., Hoffman, F.M., Thornton, P.E., Mahowald, N.M., Lindsay, K., Lee, Y.-H., Nevison, C.D., Doney, S.C., Bonan, G., Stöckli, R., Covey, C., Running, S.W., Fung, I.Y., 2009. Systematic assessment of terrestrial biogeochemistry in coupled climate–carbon models. *Global Change Biology* 15, 2462–2484. <https://doi.org/10.1111/j.1365-2486.2009.01912.x>
- Reid, C.E., Brauer, M., Johnston, F.H., Jerrett, M., Balmes, J.R., Elliott, C.T., 2016. Critical Review of Health Impacts of Wildfire Smoke Exposure. *Environmental Health Perspectives* 124, 1334–1343. <https://doi.org/10.1289/ehp.1409277>
- Reid, C.E., Considine, E.M., Maestas, M.M., Li, G., 2021. Daily PM_{2.5} concentration estimates by county, ZIP code, and census tract in 11 western states 2008–2018. *Sci Data* 8, 112. <https://doi.org/10.1038/s41597-021-00891-1>
- Rhoades, C.C., Fornwalt, P.J., 2015. Pile burning creates a fifty-year legacy of openings in regenerating lodgepole pine forests in Colorado. *Forest Ecology and Management* 336, 203–209. <https://doi.org/10.1016/j.foreco.2014.10.011>
- Rooney, B., Wang, Y., Jiang, J.H., Zhao, B., Zeng, Z.-C., Seinfeld, J.H., 2020. Air quality impact of the Northern California Camp Fire of November 2018. *Atmospheric Chemistry and Physics* 20, 14597–14616. <https://doi.org/10.5194/acp-20-14597-2020>
- Shi, L., Zanobetti, A., Kloog, I., Coull, B.A., Koutrakis, P., Melly, S.J., Schwartz, J.D., 2016. Low-Concentration PM_{2.5} and Mortality: Estimating Acute and Chronic Effects in a Population-Based Study. *Environ Health Perspect* 124, 46–52. <https://doi.org/10.1289/ehp.1409111>
- Stephens, S.L., Martin, R.E., Clinton, N.E., 2007. Prehistoric fire area and emissions from California’s forests, woodlands, shrublands, and grasslands. *Forest Ecology and Management* 251, 205–216. <https://doi.org/10.1016/j.foreco.2007.06.005>
- Sutherland, S., and Edwards, E., 2022. Does Environmental Review Worsen the Wildfire Crisis? How environmental analysis delays fuel treatment projects. Retrieved from <https://hdl.handle.net/10161/25599>.
- Torres, O., Jethva, H., Ahn, C., Jaross, G., Loyola, D.G., 2020. TROPOMI aerosol products: evaluation and observations of synoptic-scale carbonaceous aerosol plumes during 2018–2020. *Atmospheric Measurement Techniques* 13, 6789–6806. <https://doi.org/10.5194/amt-13-6789-2020>
- US Department of Agriculture Forest Service, 2009. Pacific Southwest Research Station General Technical Report PSW-GTR-224.
- US EPA, 2021. Comparative Assessment of the Impacts of Prescribed Fire Versus Wildfire (CAIF): A Case Study in the Western U.S. U.S. Environmental Protection Agency, Washington, DC, EPA/600/R-21/197, 2021.
- Vaillant, N.M., Fites-Kaufman, J.A., Stephens, S.L., 2009. Effectiveness of prescribed fire as a fuel treatment in Californian coniferous forests. *Int. J. Wildland Fire* 18, 165–175. <https://doi.org/10.1071/WF06065>
- van der Werf, G.R., Randerson, J.T., Giglio, L., van Leeuwen, T.T., Chen, Y., Rogers, B.M., Mu, M., van Marle, M.J.E., Morton, D.C., Collatz, G.J., Yokelson, R.J., Kasibhatla, P.S.,

- 942 2017. Global fire emissions estimates during 1997–2016. *Earth System Science Data* 9,
943 697–720. <https://doi.org/10.5194/essd-9-697-2017>
- 944 Wang, Q., Jacob, D.J., Fisher, J.A., Mao, J., Leibensperger, E.M., Carouge, C.C., Le Sager, P.,
945 Kondo, Y., Jimenez, J.L., Cubison, M.J., Doherty, S.J., 2011. Sources of carbonaceous
946 aerosols and deposited black carbon in the Arctic in winter-spring: implications for
947 radiative forcing. *Atmospheric Chemistry and Physics* 11, 12453–12473.
948 <https://doi.org/10.5194/acp-11-12453-2011>
- 949 Wu, Y., Cordero, L., Gross, B., Moshary, F., Ahmed, S., 2012. Smoke plume optical properties
950 and transport observed by a multi-wavelength lidar, sunphotometer and satellite.
951 *Atmospheric Environment* 63, 32–42. <https://doi.org/10.1016/j.atmosenv.2012.09.016>
- 952 Yang, Q., Yuan, Q., Li, T., Yue, L., 2020. Mapping PM_{2.5} concentration at high resolution using
953 a cascade random forest based downscaling model: Evaluation and application. *Journal of*
954 *Cleaner Production* 277, 123887. <https://doi.org/10.1016/j.jclepro.2020.123887>
- 955 Yue, X., Mickley, L.J., Logan, J.A., Kaplan, J.O., 2013. Ensemble projections of wildfire
956 activity and carbonaceous aerosol concentrations over the western United States in the
957 mid-21st century. *Atmos Environ* (1994) 77, 767–780.
958 <https://doi.org/10.1016/j.atmosenv.2013.06.003>